Response of magnesium single crystals to shock-wave loading at room and elevated temperatures

2014 J. Phys.: Conf. Ser. 500 112027

(http://iopscience.iop.org/1742-6596/500/11/112027)

Journal of Physics: Conference Series **500** (2014) 112027 doi:10.1088/1742-6596/500/11/112027

Response of magnesium single crystals to shock-wave loading at room and elevated temperatures.

G V Garkushin[1], A S Savinykh[1], G I Kanel[2], S V Razorenov[1], D Jones[3], W G Proud[3] and L R Botvina[4]

[1] Institute of Problems of Chemical Physics of RAS, Chernogolovka, 142432 Russia
[2] Joint Institute for High Temperatures of RAS, Izhorskaya 13, Moscow, 125412 Russia
[3] Institute of Shock Physics, Imperial College London, London, SW7 2AZ, UK
[4] Institute of Metallurgy and Material Science of RAS, Leninsky 49, Moscow, 119991 Russia

E-mail: garkushin@icp.ac.ru

Abstract. A series of magnesium single crystals, from 0.2 to 3 mm thick, were shock loaded along specific axes, a and c, of the hexagonal closed packed (hcp) structure. Other experiments involved loading at 45 degrees to these principal axes. Shock compression along the *c*-axis causes inelastic deformation by means of pyramidal slip and twinning and is associated with the largest Hugoniot elastic limit (HEL) for this material. The low-energy basal slip was activated by shock loading along the inclined direction and has he smallest HEL. In all cases, we observe the decay of the elastic precursor wave and growth of the HEL with increasing temperature. For the c-orientation this change is caused by a decrease of elastic constants, not an increase of shear stress along the pyramidal slip planes. For the other orientations the shear stress on the slip planes increased with temperature. For the inclined shock compression, after the HEL, two plastic waves were found: the stress level of the first plastic wave depends on the ultimate shock stress. Finally, the largest spall strength was along the a-axis and the smallest in the off-axis direction.

1. Introduction

Shock-wave studies of dynamic yielding and fracture of metal single crystals have been performed on face-centred cubic (fcc) metals such as copper [1] and aluminium [2], body-centred cubic (bcc) metals such as molybdenum [3], hexagonal close-packed (hcp) *e.g.* beryllium [4] and zinc [5]. Shock studies with aluminium and zinc single crystals have been performed over a wide range of temperatures. In the case of aluminum, these have revealed an anomalous growth of the dynamic yield stress with temperature. This effect can be explained by a large contribution of phonon friction to the dislocation drag at high strain rates but this explanation still needs more investigation. This trend is not found in zinc single crystals. Here, impact in the low elastic modulus (0001) basal plane, no elastic precursor wave was observed. Shock loading of beryllium single crystals in off-axis directions [4] resulted in formation of multiple plastic shock waves only some of which were predicted by theory [6].

The main aim of this study is to find materials with slip directions where the anomalous growth of the dynamic yield stress may be observed. Magnesium was selected for a number of reasons. The

deformation systems in magnesium are governed by its hcp crystal structure with a length ratio $r=c/a=1.624$. It has three well-known slip systems: basal, prismatic, and pyramidal. Twinning makes a large contribution to the deformation process if basal slip is hampered. Most importantly, for this study, depending on the crystal orientation with respect to shock loading, it is possible to study the dynamic yield of each system separately. Basal slip should be observed for shock loading in directions inclined to the *c* axis. Prismatic slip is activated for wave propagation along the *a* axis or in any other transverse direction where the primary, prismatic, system not subject to shear stress. Finally, pyramidal slip and twinning should be activated for wave propagation along the *c* axis. Thus, there is opportunity to study several deformation mechanisms independently. In analyzing the shock-wave data, it is important to know the temperature dependences of the elastic constants, these are known both from experiments [7] and *ab initio* calculations [8]. Finally, magnesium and its alloys are widely used and there are several publications *e.g.* [9] on their shock behaviour.

2. Material and experiments

All samples were cut from rod, 10 mm in diameter, sample thickness was varied from 0.2 mm to 3 mm. The samples were ground and polished and were chemically treated following annealing at 723 K for 25 min. Shock loading of the samples was carried out along the *c* and *a*-axis direction, and in the direction at 45 degrees to the *c*-axis. Shock waves were generated by plate impact using aluminium flyer plates of 0.2 mm, 0.4 mm, 0.85 mm and 2.0 mm thickness at a velocity of 630±30 m/s. These flyers were explosively launched. Experiments were heated using resistive heaters operating at up to 1 kW. Samples heated in this way reached the required temperature within 10 min. The temperature was monitored and controlled using thermocouples, giving ±10°C accuracy. The free surface velocity of the sample was monitored using VISAR [10].

3. Results and Discussion

Figure 1 presents an example of the free surface velocity history measured for 2.0-mm-thick sample impacted at 0.63±0.03 km/s along the *c*-axis by a 0.37 mm thick aluminium flyer plate.

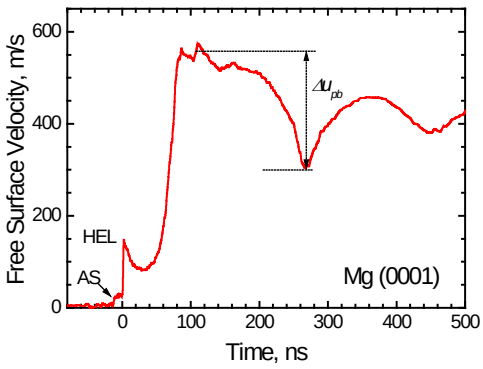

Figure 1. Free surface velocity of 2.0-mm-thick magnesium single crystal. The (0001) orientation was impacted by an aluminum flyer plate, 0.37 mm thick, at 0.66±0.03 km/s. The small feature 'AS' is the air shock in front of the flyer plate.

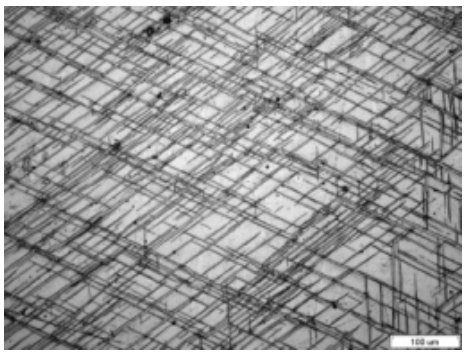

Figure 2. Microstructure of Mg single crystal samples of *c*-orientation recovered after shock loading.

In figure 1, the compressive part of the waveform is very similar to that for beryllium in *c*-orientation. The wave shows an elastic precursor wave followed by a plastic shock wave. The rise time of the spike-like precursor wave front is less than 1 ns. Precursor waveforms with spikes are usually associated with accelerating stress relaxation as described in [11]. The waveform shows irregular oscillations at the top of shock pulse often accompany twinning, as reported in *e.g.* [12]. Tensile stresses are generated inside the sample after reflection of the compression pulse from the free surface.

If the tensile stress reaches a critical magnitude, a spall fracture is initiated within the sample and the "spall pulse" appears in the free surface velocity profile. The fracture strength of the material is determined from the velocity pullback from the peak value to the value right ahead of the spall pulse, Δu_{fs}. The oscillations seen later in the trace, are caused by wave reverberation in the spalled layer.

Figure 2 shows optical micrograph of the (0001) plane of the crystal 0.31 mm below the impact surface and shows intense pyramidal twinning. Twins occupy up to 35% of the micrograph area.

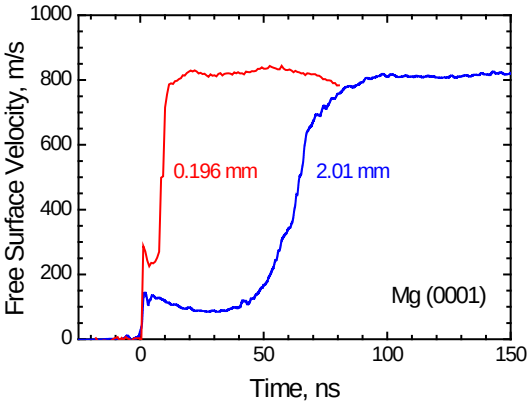

Figure 3. Decay of the elastic precursor wave in Mg single crystal, orientated (0001), impacted by a 2 mm Al flyer plate through a 2-mm-thick Al base plate.

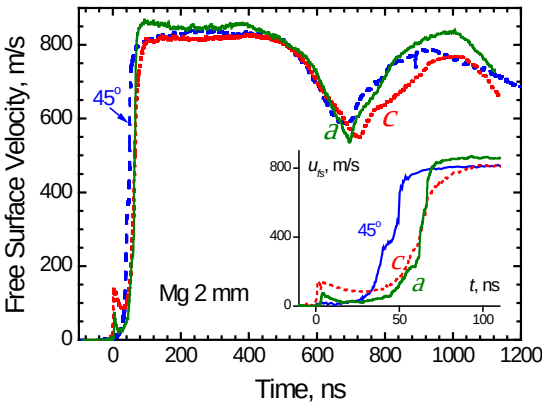

Figure 4. Free surface velocity histories of 2-mm-thick Mg single crystal samples shocked along the three different orientations.

Figure 3 shows evolution of shock wave in *c*-oriented crystal at its propagation from 0.196 mm to 2.01 mm distance. A two-fold decrease in the peak stress of the elastic precursor wave and a significant increase of the rise time of plastic shock wave are seen.

In figure 4 the waveforms measured for shock loading along the *c*-axis, *a*-axis and at 45° with respect to the *c*-axis are compared. As was expected, the slip along inclined basal (0001) plane occurs at lowest shear stress and this also gives the lowest HEL value of the orientations. The relatively large rise time of the elastic precursor front requires additional care in determining the HEL value. The waveforms in figure 4 clearly demonstrate variations of the resistance to spall fracture with varying the impact direction. A more interesting observation is that the plastic shock wave splits in two waves with different propagation velocities. The later is clearly seen in figure 5 where evolution of shock wave as it propagates through inclined crystal is presented.

Such splitting of the plastic shock wave was observed in experiments with beryllium single crystals [4] and is not predicted using the theory of plane wave propagation in anisotropic elastic-plastic solids [6].

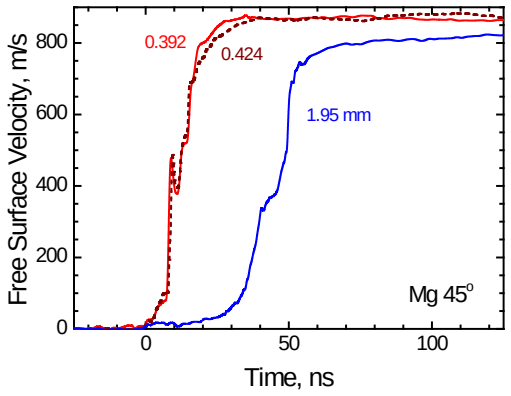

Figure 5. Decay of the elastic precursor wave in Mg single crystal for shock loading at 45° with respect to the c-axis.

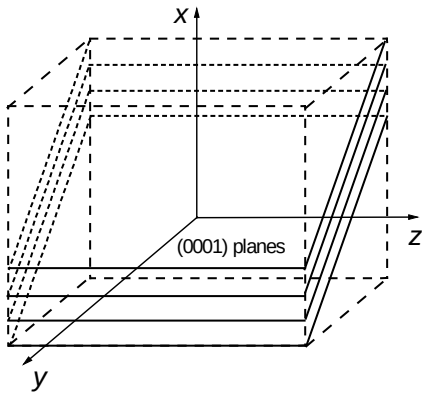

Figure 6. Scheme of plastic slip in the case of shock loading at 45° with respect to the c-axis.

It is possible that the appearance of the step in plastic shock wave is caused by activation of higher order slip systems. In uniaxial compression in the *c* direction (direction *x* in figure 6), the slip along the inclined (0001) planes may provide relaxation of the deviatoric stresses in the *x*- and *y*-directions but cannot provide relaxation of the *z*-component. As a result, the stress difference $\sigma_x - \sigma_z$ continues to grow even as the (0001) slip system: the secondary slip system becomes active when the $\sigma_x - \sigma_z$ value becomes large enough. Overall, the relaxation of lateral stress components do not take place under uniaxial stress condition but arise, instead under uniaxial strain. This conclusions needs further validation.

Figures 7 and 8 illustrate influence of the temperature on the HEL and spall strength values for two impact directions. In both cases the HEL grows with increasing temperature. However, since the elastic constants also depend on temperature, the yield stress (Y) and the resolved shear stress (τ) in slip planes decreases with temperature at shock loading along the *c*-axis.

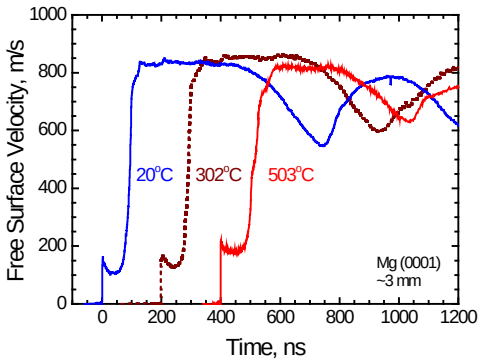

Figure 7. The free surface velocity histories of *c*-oriented 3-mm crystal samples at three different temperatures.

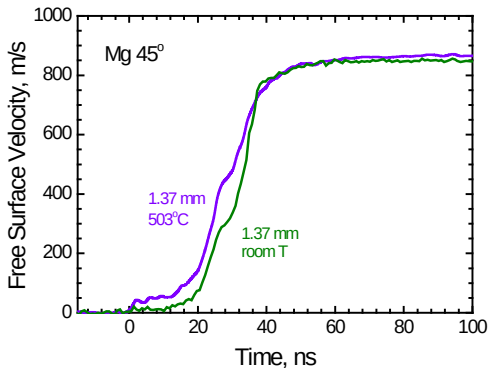

Figure 8. Front part of the waveforms measured for 1.4 mm thick samples with 45° orientation tested at two temperatures.

For shock loading in the inclined direction, Y and τ grow with increasing the temperature, but the overall values themselves are small. This difference is treated in terms of relatively small contribution of the phonon friction F when it is much lower the resolved shear stress, $F << \tau$, for shock

compression along the *c*-axis and the relatively large contribution when $F \approx \tau$ for shock compression in the inclined direction. The spall strength decreases with heating in all cases. Table 1 summarises results of treatment of the experimental data.

Table 1. Results of measurements of dynamic flow stress and spall strength.

Figure	Plane	T °C	Sample (mm)	Impactor (mm)	σ_{HEL} (GPa)	Y (GPa)	τ (GPa)	σ_{sp} (GPa)	Spall (mm)
3	$(10\bar{1}0)$	23	1.98	0.37/0	0.89 0.165	0.545 0.1		1.28	0.32
3		23							
5	(0001)	23	0.196	1.94/1.91	1.49 1.23				
5	(0001)	23	2.01	2.07/1.88	0.72 0.43			1.36	1.61
7	45°	23							
7	45°	23	1.95	1.98/2.0	0.09			1.25	1.54
	(0001)	23	3.03	2.05/2.05	0.78 0.55	0.5	0.23	1.41	1.5
	(0001)	302	3.23	2.05/1.99	081 0.63	0.49	0.22	1.18	1.5
	(0001)	503	3.25	1.98/1.92	0.96 0.82	0.48	0.23	0.85	1.2

Acknowledgements
Funding was provided by the Russian fund of basic researches, Grant 11-02-01141-a. The authors thank Ermolov L.G. for providing the experiments. The Institute of Shock Physics acknowledges the support of the Atomic Weapons Establishment, Aldermaston, United Kingdom and Imperial College London.

References
[1] Jones O E and Mote J D 1969 *J. Appl. Phys.* **41** 2330
[2] Kanel G I and S V Razorenov 2001 *Phys. Solid State*. **43** 871
[3] Kanel G I *et al.* V 1993 *J. Appl. Phys.* **74** 7162
[4] Pope L E and Johnson J N 1975 *J. Appl. Phys*. **46** 720
[5] Bogach A A *et al.* 1998 *Phys. Solid State* **40** 1676
[6] Johnson J N 1972 *J. Appl. Phys.* **43** 2074
[7] Slutsky L J and Garland C W 1957 *Phys. Rev.* **107** 972
[8] Greeff C W and Moriarty 1999 *J. Appl. Phys. Rev*. B **59** 3427
[9] Kanel G I, Razorenov S V, Bogatch A A and Utkin A V *et al* 1996 *J. Appl. Phys.* **79** 8310
[10] Barker L M and Hollenbach R E 1972 *J. Appl. Phys*. **43** 4669
[11] Kanel G I, Razorenov S V and Fortov V E 2004 *Shock-Wave Phenomena and the Properties of Condensed Matter* (Springer New York) 320
[12] Razorenov S V *et al.* 2005 *Phys. Solid State* **47** 663